

# Weldment properties evaluation and formability study of tailor-welded blanks of different thickness combinations and welding orientations

C. H. Cheng · L. C. Chan · C. L. Chow

Received: 5 March 2006 / Accepted: 10 October 2006 / Published online: 6 April 2007  
© Springer Science+Business Media, LLC 2007

**Abstract** Tailor-welded Blanks (TWBs) are tailor-made for different complex component designs by welding multiple metal sheets with different thicknesses, shapes or strengths prior to forming. However, the forming performance of an intrinsic TWB is critically related to its own structures and designs, such as the thickness combination, as well as the location and orientation of weldment. In this study, a 2 kW Nd:YAG laser were used to butt-weld approximately 180 samples of stainless steel (AISI 304) TWBs with different dimensions (i.e., from 12.7 mm to 165.1 mm in width), thickness combinations (i.e., 1.0/1.0 mm, 1.0/1.2 mm, 1.0/1.5 mm, 1.2/1.2 mm, 1.2/1.5 mm and 1.5/1.5 mm) and welding orientations (i.e., 0°, 45° and 90°). Subsequently, Swift forming tests were carried out to characterize the forming performance of those TWBs. Obviously, the optimal sets of welding parameters relating critically to the quality of weld was a primary criterion for the formability test of TWBs in this study. The effects of different thickness combinations on the formability of TWBs were investigated through the constructed forming limit diagrams (FLDs). The results showed that the thinner part of TWBs dominated the majority of deformation similar to the FLD of the parent metal. The effects of different welding orientations on the forming performance of TWBs were examined from the failure analysis.

## Introduction

The use of tailor-welded blanks (TWBs) has been increasingly employed in the automotive industry and extended to other potential industrial applications, such as electrical goods, package and construction markets [1]. As TWBs are usually tailor-made for different components, the forming performance of the TWBs is a major industrial concern. As most of the TWBs have been produced with laser welding, the quality of weld is considered a major factor governing the reliability of TWBs, as well as their forming performance [2]. A poor quality of weld with defects or cracks has often led to initiation of weld failure, which in turn causes unexpected failure of TWB during forming. The weldment in steel TWB has been found to be in general stronger than its base metal [3, 4]. Possible reason for enhanced tensile strength of the welded metal is the presence of coarser and larger grains of welded metal [5]. However, this coarse grains decrease the ductility and toughness of the welded metal. Some researchers [5–7] studied the direct relationship between welding parameters and formability of TWBs. In the experiments carried out by Eisenmenger and Bhatt [6], it was found that the formability of TWBs increased with increased welding speed or decreased laser power for obtaining a narrow weldment with full penetration using the minimum input energy. However, high speed welding may cause welding defects such as oxide inclusions in the welded metal [5]. Radlmayr and Sziyur [8] reported that shielding gas, focus position of laser beam and workpiece alignment are also the main factors affecting the quality of weld and the formability of TWBs.

In recent years, researchers have analyzed the forming performance of steel TWBs using different tests. Saunders and Wagoner [7] have identified two failure modes of

---

C. H. Cheng · L. C. Chan (✉)  
Department of Industrial and Systems Engineering,  
The Hong Kong Polytechnic University, Hung Hom,  
Kowloon, Hong Kong, China  
e-mail: mflcchan@inet.polyu.edu.hk

C. L. Chow  
Department of Mechanical Engineering, University of Michigan-  
Dearborn, 4901 Evergreen Road, Dearborn, MI, USA

TWBs and reported that the press formability of TWBs relating to the changing deformation patterns depended on the differential strength of TWBs. The first type of failure occurred across the weldment was caused by the higher strength and lower elongation of the weld. This failure would most likely occur when the major strain direction was parallel to the weldment subjecting base metals and weldment to the same loads. The second failure type occurred in the weakest base metal. This would occur when the major strain direction was perpendicular to the weldment, forcing the weaker base metals to be stretched while the weldment acted as a non-deformable material. Heo et al. [9] indicated that a higher thickness strain distribution led to a larger movement of weld line during deep drawing. Also, Chan et al. [10] claimed that the formability of TWB decreased against the increase of the thickness ratio of a TWB.

In this paper, an effective laser-welding process of stainless steel (AISI 304) TWBs with different welding orientations and thickness combinations is presented, while the effects of welding orientation and thickness combination on the formability of TWBs are also investigated.

### Preparation of quality laser-welded TWBs

In order to carry out a reliable formability analysis on TWBs, well-preparation of laser-welded TWBs with quality welds is necessary, an essential pre-condition for the formability test in this study. Before the formability test, the experimental procedures of laser welding process should be clearly illustrated, while optimal sets of laser-welding parameters, which provide each TWB a quality weld, should be firstly identified and assessed by several examinations on those welds.

In this study, AISI 304 stainless steel TWBs were butt-welded using a 2 kW Nd:YAG laser. Three stainless steel sheets with thicknesses of 1, 1.2 and 1.5 mm were used to produce approximately 180 samples of TWBs having different welding orientations (i.e., 0°, 45° and 90°) and thickness combinations (i.e., 1.0/1.0 mm, 1.0/1.2 mm, 1.0/1.5 mm, 1.2/1.2 mm, 1.2/1.5 mm and 1.5/1.5 mm). Before the laser welding, the edges of the specimens to be welded were milled and degreased to attain clean edges without any burrs, contaminates, or oils. Each pair of specimens was assembled on a welding fixture for laser-beam alignment and specimen fit-up, as shown in Fig. 1. Welding trials on TWBs were carried out for each thickness combination using various laser powers, welding speeds, focusing positions of laser beam and flow-rates of shielding gas. After extensive welding trials, the optimal welding parameters of TWBs for each thickness combinations were identified to be described in a later section. In accordance

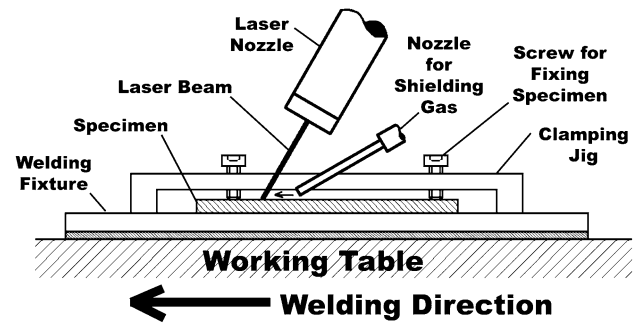


Fig. 1 Schematic diagram of the welding setup

with the British Standards EN ISO 13919-1 [11] and 15614-11 [12], the weld integrity was examined with respect to the conditions of weld surface and cross-sectional weld profile, while the general mechanical properties of the TWBs were measured using the tensile test.

### Formability test of TWBs

The formability of the TWBs was examined by means of the measured dome heights from Swift forming test. In addition, the forming limits in terms of the major and minor strains of the TWBs with varying widths were measured, whilst the forming behavior and the failure modes of the specimens were also investigated. With the aids of these test results, the effects of every welding orientation and the thickness ratio were analyzed accordingly. Despite different orientations, almost all the welds were located in the middle of TWBs, as shown in Fig. 2. A forming tester with a hemispheric punch (50 mm in diameter) was used while a large blank-holding force of 100 kN was applied to control the material flow. In order to balance the thickness difference within a TWB, tailor-made spacers were designed and applied during the test.

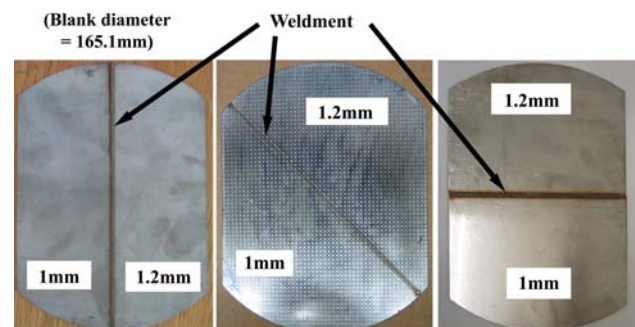


Fig. 2 TWBs with different welding orientations (a) 0° (b) 45° (c) 90°

## Results and discussions

Weldment properties evaluation—a pre-condition for formability test

### Optimal sets of welding parameters

AISI 304 stainless steel TWBs with different welding orientations (i.e.,  $0^\circ$ ,  $45^\circ$  and  $90^\circ$ ), thickness combinations (i.e., 1.0/1.0 mm, 1.0/1.2 mm, 1.0/1.5 mm, 1.2/1.2 mm, 1.2/1.5 mm and 1.5/1.5 mm) and specimen widths (i.e., from 12.7 mm to 165.1 mm) were produced using the 2 kW Nd:YAG laser. After extensive trials, the optimal sets of welding parameters for welding TWBs with different thickness combinations were identified and listed in Table 1. Several typical samples are shown in Fig. 2. It is apparent that the optimal welding parameters can be achieved by selecting an appropriate welding speed according to the total thickness of base metals on both sides of TWB. In general, a lower welding speed should be chosen for thicker material, whereas the laser power could be fixed within a narrow range from 1,000 W to 1,100 W. For all the thickness combinations, the laser beam was focused on the joint of the top surface of the specimen or the thicker base metal while Argon gas with a flow rate of 20 L/min was used for shielding.

Figures 3 and 4 show, respectively, the weld surface and the cross-sectional weld profile obtained from a TWB (i.e., 1.0/1.2 mm) welded using a set of the optimal parameters. The weld surface was found clean and continuous

**Table 1** Optimal welding parameters

Thickness combination	Laser power (W)	Welding speed (mm/s)	Focus	Shielding gas
1/1 mm	1,100	27	Surface	Argon (20 l/min)
1.2/1.2 mm	1,000	23		
1.5/1.5 mm	1,100	15		
1/1.2 mm	1,000	25	Surface of thicker base metal	
1/1.5 mm	1,100	20		
1.2/1.5 mm	1,100	15		



**Fig. 3** Weld surface of TWB produced under optimal parameters

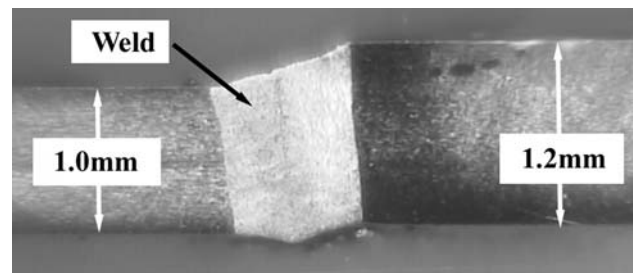


**Fig. 4** Cross-sectional weld profile of TWB produced under optimal parameters

throughout the entire length of the TWB without any visible cracks or porosity, while an acceptable weld profile was attained without any defect such as underfill, undercut or weld-sagging. The tensile properties of the TWBs with different thickness combinations of transversal welds were evaluated under the ASTM Standard E 8M [13]. The tensile test was carried out under a constant cross-head speed of 1 mm/min until the initiation of localized necking. As shown in Fig. 5, most failures were typically found in the base metal rather than the weld or the heat-affected zone (HAZs). According to the guidelines reported in Ref. [14], both the welds and TWBs, which were produced based on the recommended set of the welding parameters are considered acceptable and of high quality.

### Tensile properties of TWBs and their weldment

In order to gain an understanding of the structural behaviors of TWBs, the tensile curves of the TWBs with different thickness combinations were measured (Fig. 6a) and compared with those of their base metals (Fig. 6b). Curves (1), (2) and (3) in Fig. 6a showed that the TWBs with similar thickness combinations (i.e., 1.0/1.0 mm, 1.2/1.2 mm and 1.5/1.5 mm) possessed similar stress and strain values as those of their base metals (i.e. curves (1), (2) and (3) in Fig. 6b). However, for the TWBs with dissimilar thickness combinations (i.e., 1.0/1.2 mm, 1.0/1.5 mm and 1.2/1.5 mm), a larger difference in thickness

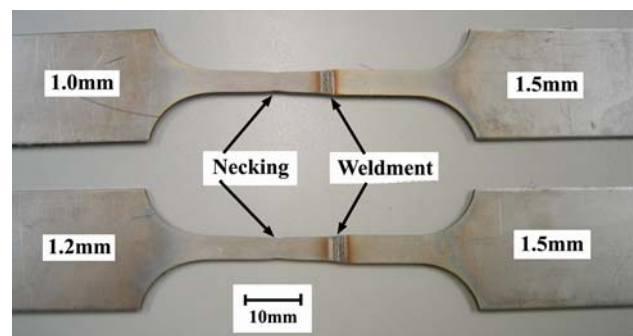


**Fig. 5** Some results of tensile test for TWBs

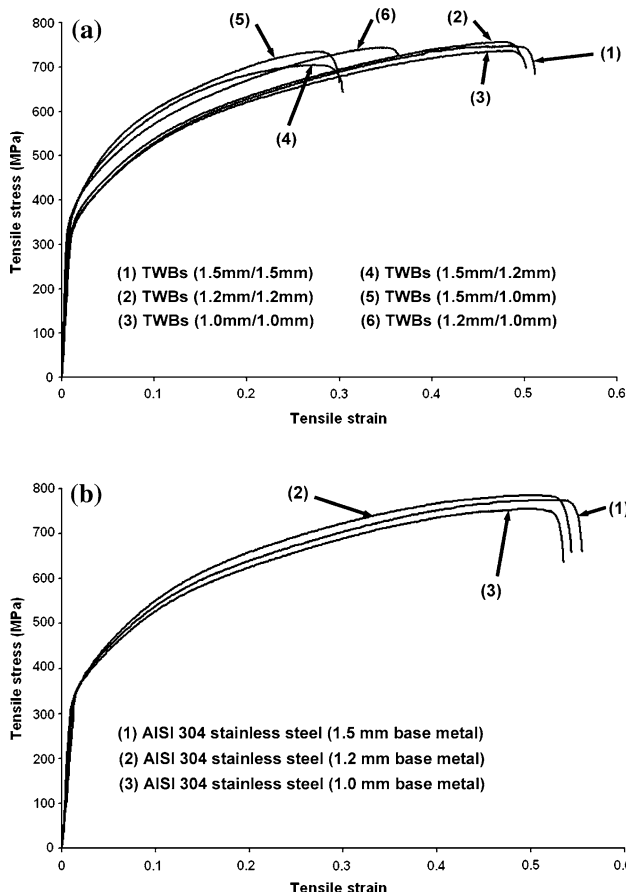


**Fig. 6** Tensile curves for (a) AISI 304 stainless steel TWBs with different thickness combinations and (b) their base metals

with the TWB resulted in lower strain values, as shown in curves (3), (4) and (5) in Fig. 6a. This was because the deformations of TWBs were as expected predominated by the thinner base metals, as shown in Fig. 5.

On the other hand, the distinctive tensile properties of weldment in the longitudinal direction were acquired using a real-time microscopic recording system presented in [15] and a specially designed tensile specimen of weldment, as shown in Fig. 7. The gauge length of the specimen contained only the weldment such that the mechanical properties of the weldment were able to be tested independently during the tensile test. With the aid of the recording system, the deformation of pre-printed grids on the surface of weldment and the tensile load applied by the tensile machine were captured and recorded simultaneously. After image analysis and evaluation of stress–strain data, the true stress–strain curve of weldment was constructed accordingly. Figure 8 shows the true stress–strain curve of weldment, i.e. Curve (1), for the TWB with a thickness combination of 1.0/1.2 mm, while Curves 2 and 3 represent the true stress–strain curves for its thinner (1.0 mm) and thicker (1.2 mm) base metals acquired using the same

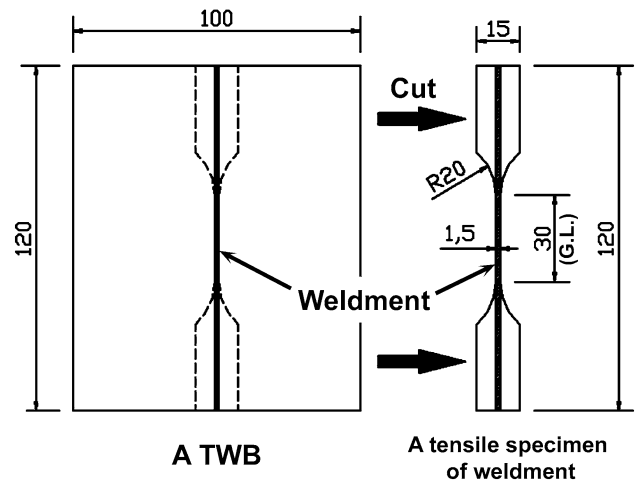


**Fig. 7** A special design of tensile specimen for weldment [15]

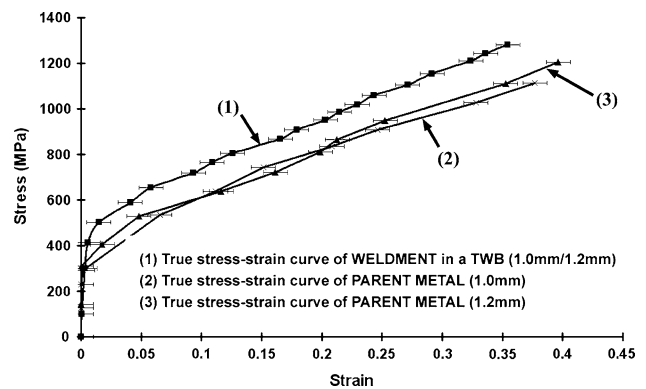


**Fig. 8** True stress–strain curves of weldment and base metals for AISI 304 stainless steel TWB [15]

recording system. The weldment is shown to possess a higher ultimate tensile strength (1,281 MPa) when compared to that of the 1 and 1.2 mm base metals (i.e., 1,112 and 1,205 MPa), respectively. The necking strain of weldment is 0.35, while that of the base metals are 0.37 (for 1.0 mm) and 0.39 (for 1.2 mm). Table 2 shows some relevant measured mechanical properties of the base metals and weldment as well as the monolithic TWB. Despite a slightly lower ductility, the weldment is found to be the strongest material comparative to all other regions in TWBs. The test results serve to illustrate why the weldment can withstand most of the applied stressing and only that minimum strain is observed in the weldment during the transverse tensile test of TWBs shown in Fig. 5.

*Microstructure and microhardness of weldment*

In order to further explain the mechanical behavior of TWBs, the microstructural analysis was carried out on

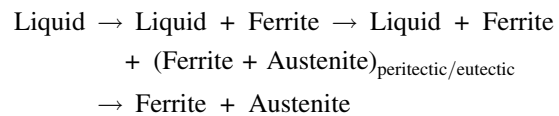


**Table 2** Mechanical properties of base metals, weldment and monolithic TWB

Material	Thickness (mm)	True yield strength (MPa)	True tensile strength (MPa)	True necking strain	Average normal anisotropy, $r_m$	Strain-hardening exponent, $n$
Base metal	1.0	355	1,112	0.37	1.0	0.45
	1.2	372	1,205	0.39	1.0	0.45
Weldment	1.0/1.2	501	1,281	0.35	–	0.48
TWB	1.0/1.2	390	1,015	0.30	–	0.46

both weldment and base metal of TWB. Figure 9a displays the microstructure of the base metal (AISI 304) consisting equiaxed austenite grains, which is a typical microstructure of a wrought austenitic stainless steel. After laser-welding, skeletal  $\delta$ -ferrite morphology in the austenitic matrix resulting from the ferrite-to-austenite transformation can be observed in the weldment, as shown in Fig. 9b. Finally, Fig. 9c depicts the fusion boundary between the weldment and base metal, where a partly melted zone is observed (indicted by the arrows) due to the change in the cellular patterns. However, no visible heat-affected zone can be found between the fusion zone and base metal.

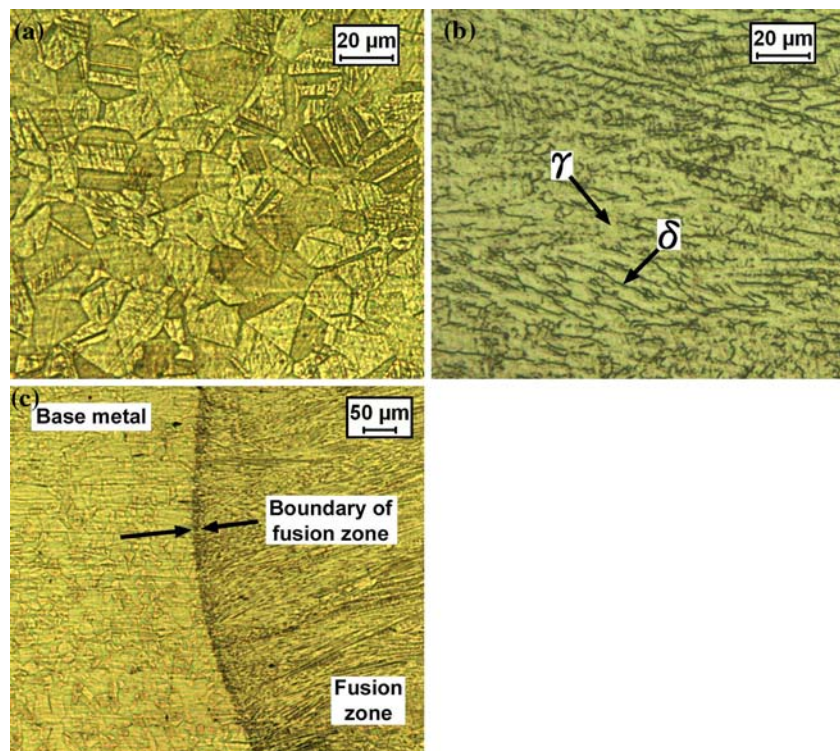
It can be concluded that the grain size of the weldment, which is predominantly austenitic before welding, has been refined due to the rapid solidification under the high cooling rate in laser-welding. The possible solid-state transformation during solidification of the welded metal upon cooling can be described as follows [16]:



The presence of ferrite in the weldment acts as a second phase-strengthening agent and increases the strength of weldment [16]. A higher level of ferrite content in weldment typically results in higher strength and lower ductility relative to the base metal. Consequently, the change in microstructure of weldment can further explain why, as shown in the stress–strain curves in Fig. 8, that the weldment possesses a relatively higher strength and a lower strain value as compared with base metal.

On the other hand, as illustrated in the schematic diagram (at the upper-right corner) in Fig. 10, the hardness variations across the cross-section of weld bead, thinner and thicker base metals were measured from the TWBs with dissimilar thickness combinations (i.e., 1.0/1.2 mm, 1.0/1.5 mm and

**Fig. 9** Microstructure of an AISI 304 stainless steel TWB at (a) base metal, (b) weldment and (c) fusion boundary



1.2/1.5 mm). As shown in Fig. 10, the hardness values of weldment (in shaded area) for all the measured TWBs are slightly higher than those of their base metals by 9–18%, whilst all the base metals (i.e., 1.0 mm, 1.2 mm and 1.5 mm) possess similar hardness values ranging from 215 HV to 225 HV. The increase in hardness of weldment may be attributed to the presence of hard  $\delta$ -ferrite (as shown in Fig. 9b) and the refinement of grains after laser-welding. However, the hardness increase of weldment is moderate such that only a minimum effect of weldment can be observed during the tensile test and forming test of TWBs. Furthermore, by comparing the curves of three different TWBs (with dissimilar thickness combinations) in Fig. 10, three weldment (in shaded area) showed nil significant variation in hardness (within 20 HV from 240 HV to 260 HV). It seems that the hardness of weldment in several TWBs with different thickness combinations is similar and, in this case, not significantly related to the thickness combinations of the TWBs. Actually, the material properties of weldment are dependent on the welding parameters and the weldability of the base metal [17]. In this study, due to a small range of thickness difference (1.0–1.5 mm) within TWBs and good laser-weldability of AISI 304 stainless steel [18], the optimal laser welding parameters for all types of TWBs do not appear to have much variation, as shown in Table 1. Therefore, the material properties of weldment are found to be similar to all types of TWBs, while the thickness combination of TWBs displays nil significant effect on the weldment itself.

Results of formability test

Failure mode

Swift forming tests were carried out to study the forming behavior of the TWBs, as well as their formability.

**Fig. 10** Microhardness distribution across weldment in TWBs with different thickness combinations

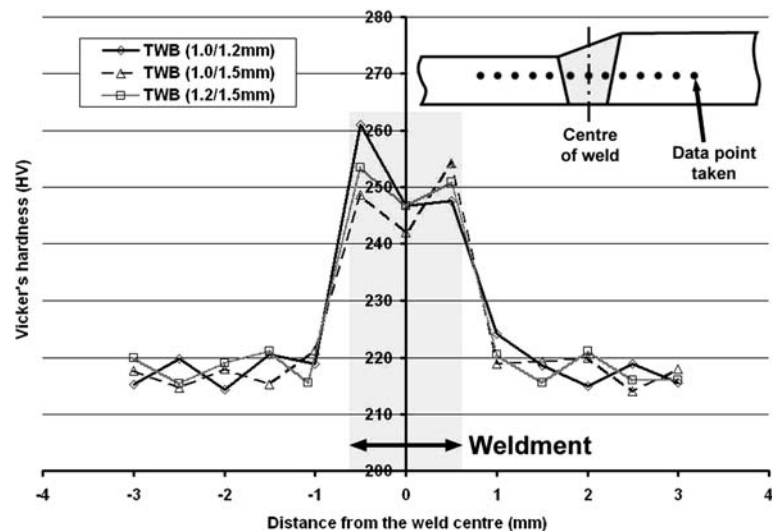
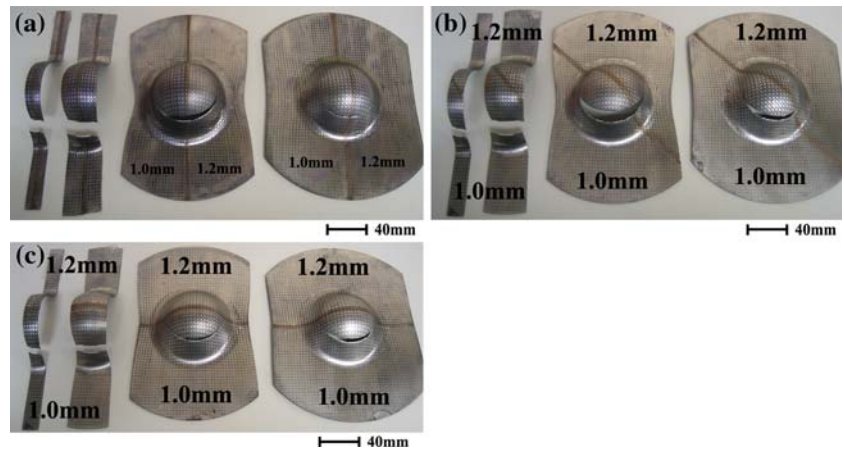


Figure 11 shows the stamped TWBs (thickness combination of 1.0/1.2 mm) with different welding orientations. It was found that the locations of failures for all the TWBs with different welding orientations were similar and all the failures propagated perpendicular to the major loading direction. Failures of TWBs with 45° and 90° welding orientations (Figs. 11b and c) were found to occur in their thinner base metal away from the weld. This phenomenon differed from those of the TWBs with 0° welds where failures initiated at the weld of (Fig. 11a). Thus, the weld orientations may be concluded to have insignificant effect on the forming behavior and the failure mode of TWBs as the failures were found to mainly occur in the thinner base metals perpendicular to the major loading direction.

Dome heights

After the Swift forming test, the dome heights of those TWBs were measured. As an example for illustration, Figs. 12 and 13 describe the measured dome heights for the TWBs of 100 mm specimen width, while the values of base metals are also plotted for comparison. It can be observed from Fig. 12 that the dome heights of TWBs with similar thickness combinations (i.e., 1.0/1.0 mm, 1.2/1.2 mm and 1.5/1.5 mm) were found to be similar in magnitude with their corresponding base metals (i.e., 1.0, 1.2 and 1.5 mm). Due to the uniform thickness throughout the entire blank, the TWBs with similar thickness combinations produced nearly identical formability and performance as their base metals during forming operation. The thicker blanks (e.g., 1.5/1.5 mm) yielded larger dome heights. The effect of minimal defects from a quality weld on the TWB forming may be considered negligible. Also, the welding orientation was found to be insignificant on the dome heights. The minor difference of dome heights observed between the TWBs with 90°, 45° and 0° welding

**Fig. 11** Formed TWBs with different welding orientations (a) 0° (b) 45° (c) 90°



**Fig. 12** Comparison of dome heights between base metals and their TWBs with similar thickness combinations

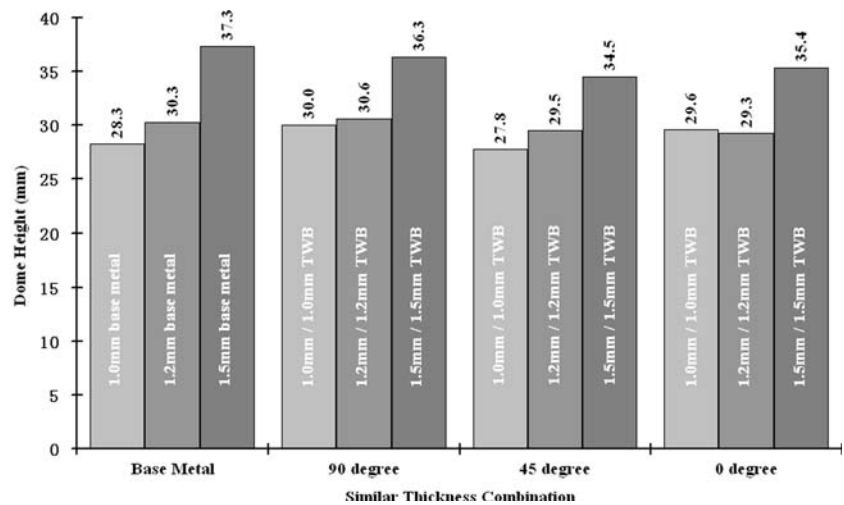
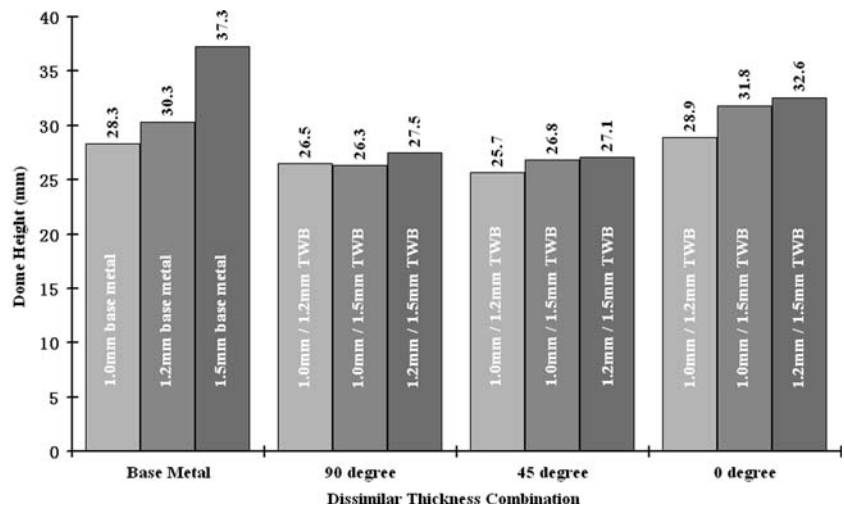


**Fig. 13** Comparison of dome heights between base metals and their TWBs with dissimilar thickness combinations



orientations are largely attributed to the variance of time interval on terminating the test immediately after the observation of failure. It can thus be concluded from this investigation that the welding orientation or TWBs with

similar thickness combinations of TWBs possess negligible effect on the formability and forming behavior of TWBs.

The dome heights of TWBs with dissimilar thickness combinations (i.e., 1.0/1.2 mm, 1.0/1.5 mm and 1.2/1.5 mm)

shown in Fig. 13 were observed on the other hand different from the base metals. For the 90° and 45° TWBs, their dome heights were obviously lower than that of base metal. Referring to the results of tensile test in Fig. 6, the difference in thickness of the intrinsic TWBs caused the uneven deformation on both thinner and thicker sides. The deformation concentrated on the thinner side generating higher stress while the thicker side may not at the same time yield any plastic deformation. As a result, the total elongation of the TWB was much lower than that of the base metal. In other words, the dome height, which reveals the overall elongation of the formed TWBs at failure, is expected to decrease accordingly. This reasonably explains why the dome heights of the TWBs with dissimilar thickness combinations are lower than the base metal. For the 0° TWBs, since the weldment was located parallel to the major loading direction during forming, both thinner and thicker sides experienced the same level of applied force along the major loading direction (Fig. 11a). Thus, the

overall elongation of the formed TWBs should be between the values of their thinner and thicker base metals. In fact, the measured dome heights of each TWB with dissimilar thickness combination were also observed to be between the range of dome heights of their thinner and thicker base metals. It can thus be concluded that the formability of the TWBs with dissimilar thickness combinations (for 90° and 45°) is much lower than that of their thinner and thicker base metals. Whilst, the 0° TWBs yields the level of formability between their thinner and thicker base metals.

*Forming limits*

In order to compare the forming limits of the TWBs relative to the base metal, the forming limits of the TWBs were constructed by measuring the major and minor strains of circular pre-printed grids on the surface of TWBs. Figures 14 and 15 show, respectively, the forming limits of TWBs (welding orientation of 90°) with both similar and

**Fig. 14** Forming limits of stainless steel TWBs (welding orientation of 90°) with similar thickness combinations

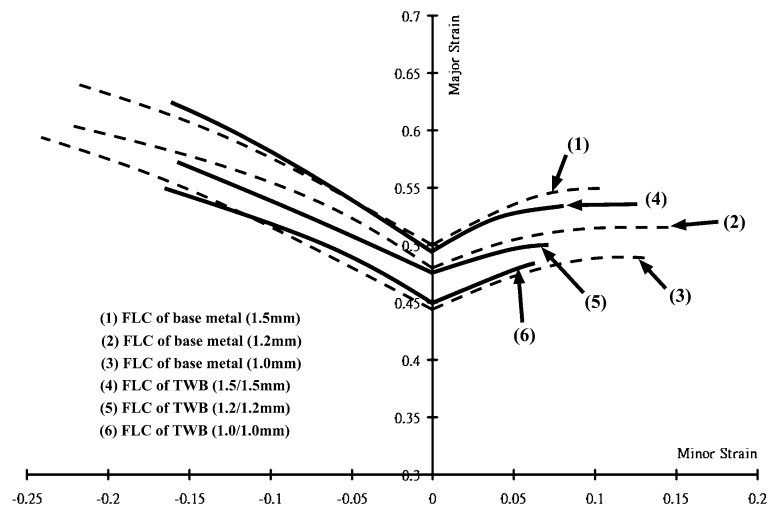
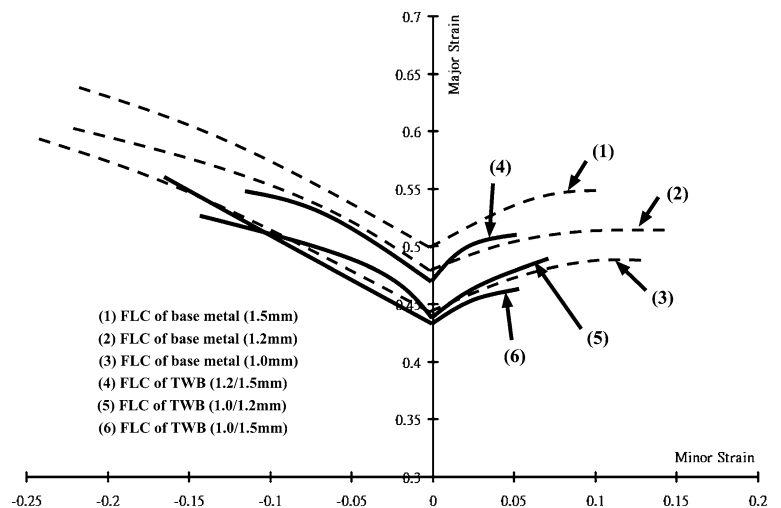


**Fig. 15** Forming limits of stainless steel TWBs (welding orientation of 90°) with dissimilar thickness combinations





dissimilar thickness combinations. Comparing to the FLDs of base metals (i.e., curves in dotted line), the TWBs with similar thickness combinations possessed similar formability as their corresponding base metals. This revealed that the weldments with 90° orientation to the major loading direction had a slight effect on the TWBs with similar thickness combinations. As shown in Fig. 11c, most of the failures in TWBs with dissimilar thickness combinations located in the thinner base metal so that similar forming limits were obtained as those of their thinner base metals.

For the forming limits of TWBs with 0° welding orientation, as shown in Fig. 11a, failures would probably initiate at the weldment or across the weldment. The construction of FLDs, therefore, becomes much more complicated whenever the distinctive formability of the weldment has to be considered. However, due to a small and indiscernible size of weldment, the fact is that, although not impossible, the experimental measurement of the forming limits of weldment is very difficult by only using existing pre-printed circular grids. Therefore, an alternative approach by combining experimental data, numerical prediction and finite element simulation is suggested to be one of the possible solutions for the formability analysis of the TWBs with 0° welding orientation. Based on the mechanical data of weldment acquired in this study and Ref. [15], the forming limit strains of weldment can be accurately predicted using a numerical method [19, 20]. Through the finite element method, the structural deformation and forming behavior of such TWBs can be simulated under the presence of weldment, while, the critical time and location of weld failure in the TWBs can be accurately predicted. Obviously, the predicted results can probably be used to enhance the formability analysis carried out in this study.

## Conclusions

In this study, AISI 304 stainless steel TWBs with different welding orientations and thickness combinations were produced using a 2 kW Nd:YAG. As the well-preparation of quality TWBs is an essential pre-condition for the formability test in this study, optimal sets of welding parameters for different thickness combinations were identified based on the weld integrity and the tensile properties of the TWBs. Similar failure modes were observed on the TWBs with different welding orientations. Once the weld quality is assured, failure generally occurs in the thinner base metal of TWBs similar to the forming limits of their corresponding thinner base metal. It is worth pointing out however that the TWB is a structure rather

than a homogeneous material like the base metal and can thus only exhibit its structural behavior. Accordingly, the dome heights were measured and used to characterize the formability of TWBs. From the measured dome height results, the TWBs with similar thickness combinations are found to yield nearly the same formability of their corresponding base metals, while the formability of TWBs with dissimilar thickness combinations decreases. It can thus be concluded that the FLDs alone are unable to fully characterize the formability of TWBs made of dissimilar thickness combinations.

**Acknowledgements** The authors would like to thank the Central Research Grant of the Hong Kong Polytechnic University for supporting this project (Project Code: R-GAP). Partial results of the paper were presented in the ‘‘LTWMP 2005 Conference’’ in May 2005 in Ukraine.

## References

1. Pallett RJ, Lark RJ (2001) *J Mater Process Technol* 117:249
2. Waddell W, Jacken S, Wallach ER (1998) SAE Technical Paper, Paper No 982396
3. Ghoo BY, Keum YT, Kim YS (2001) *J Mater Process Technol* 113:692
4. Abdullah K, Wild PM, Jeswiet JJ, Ghasempour A (2001) *J Mater Process Technol* 112:91
5. Jian X (1998) In: Laser welding of sheet metals. PhD thesis, UMI Company, Ann Arbor, Michigan
6. Eisenmenger M, Bhatt KK (1995) *Automotive Stamping Technol* 27:171
7. Saunders FI, Wagoner RH (1996) *Metall Mater Trans A-Phys Metall Mater Sci* 27A:2605
8. Radlmayr KM, Sziyur J (1991) In: Proceedings of IDDRG Working Group Meeting
9. Heo Y, Choi Y, Kim HY, Seo D (2001) *J Mater Process Technol* 111:164
10. Chan SM, Chan LC, Lee TC (2003) *J Mater Process Technol* 132:95
11. British Standard EN ISO 13919-2 (2001)
12. British Standard EN ISO 15614-11 (2002)
13. ASTM Standard E 8M (2001)
14. Tailor welded blank acceptance guidelines, Auto/Steel Partnership (1995)
15. Cheng CH, Chan LC, Chow CL, Lee TC (2005) In: Proceedings of the 2nd International Conference of Laser Technologies in Welding and Materials Processing. Crimea, p 171
16. Lippold JC, Kotecki DJ (2005) In: Welding metallurgy and weldability of stainless steels. John Wiley & Sons, New Jersey, p 153
17. Noble DN (1990) In: ASM Handbook volume 6 welding, brazing, and soldering. ASM International, Ohio, p 471
18. Duley WW (1999) In: Laser welding. John Wiley & Sons, Canada, p 26
19. Chow CL, Jie M, Hu SJ (2003) *J Eng Mater Technol Trans ASME* 125:260
20. Chan LC, Cheng CH, Jie M, Chow CL (2005) *Int J Damage Mech* 14:83